JMEPEG (2009) 18:1201–1208
DOI: 10.1007/s11665-009-9364-3

1059-9495/$19.00

Investigation of Process Parameters for the Backward Extrusion of Arbitrary-Shaped Tubes from Round Billets Using Finite Element Analysis

K. Abrinia and S. Orangi

(Submitted March 13, 2008; in revised form December 18, 2008)

Process simulation for the backward extrusion of internally arbitrary-shaped tubes from circular billets is presented in this article. ABAQUS/Explicit finite element method has been used to analyze the problem. This kind of analysis has been done before using analytical methods such as the upper bound theorem. However, the FEM solution presented here is the first of its kind. Values of stress, strain, and spatial velocity at different points in the deformation field were obtained. To observe the flow of the material during the process, grid deformations were also produced for the backward extrusion using the FEM package. Circular shape for the initial billet and arbitrary shapes for the final tube's cross sections were considered and FEM solutions were given for each. The shapes considered were elliptical, rectangular, and circular-shaped tubes and circular billets. The variation of extrusion load for the backward extrusion process was obtained for different values of reduction of area, aspect ratio, and friction factor. Also, the effect of these parameters on velocity field and free surface configuration were investigated in this simulation. The results produced from this work were compared with the theoretical and experimental results of other workers and good agreements were observed and some improvements in some of the results were also seen.

Keywords arbitrary shaped tube, backward extrusion, finite element method, round billets

1. Introduction

One of the important bulk forming processes which has a lot of applications is the backward extrusion that has been the subject of study of researchers for many years. This process is very useful for making shaped sections with closed ends or integrated parts which are difficult to produce by means of other processes. Bae and Yang (Ref 1) gave an account of an upper-bound method to determine the final-stage extrusion load and the deformed configuration for the three-dimensional backward extrusion of internally elliptic-shaped tubes from round billets. In another article, Bae and Yang (Ref 2) presented a simple kinematically admissible velocity field for the backward extrusion of internally circular-shaped tubes from arbitrarily shaped billets. They carried out experiments with full-annealed aluminum alloy billets at room temperature using four circular-shaped punches.

Another new kinematically admissible velocity field was proposed by Bae and Yang (Ref 3) to determine the final-stage extrusion load and the average extruded height in the backward extrusion of internally nonaxisymmetric tubes from round billets.

K. Abrinia and **S. Orangi**, Faculty of Mechanical Engineering, College of Engineering, University of Tehran, Tehran, Islamic Republic of Iran. Contact e-mail: cabrinia@ut.ac.ir.

Lee and Kwan (Ref 4) presented a modified kinematically admissible velocity field for the backward extrusion of internally circular-shaped tubes from arbitrarily shaped billets. From the proposed velocity field, the upper-bound extrusion load and average extruded height for regular polygonal-shaped billets were determined with respect to the chosen parameters. A new upper-bound elemental method was proposed by Lin and Wang (Ref 5) to improve the ineffectiveness of the upper bound elemental technique (UBET) for solving forging problems that were geometrically complex or needed a forming simulation for predicting the profile of the free boundary.

An upper-bound formula was developed to analyze the backward extrusion forging of regular polygon cup-shaped components in an article by Moshksar and Ebrahimi (Ref 6). Guo et al. (Ref 7) analyzed two- and one-way axisymmetric hot backward extrusion problems by a combined finite element method. A finite element simulation for the backward extrusion of internally hollow circular sections from polygonal billets was performed by Abrinia and Orangi (Ref 8). In this article, investigation of process parameters for the backward extrusion of arbitrary-shaped tubes from round billets was carried out using finite element approach.

2. FEM Simulation

A finite element analysis was used to simulate the backward extrusion of internally elliptic, rectangular, and hexagonal sections from circular billets.

Commercial pure aluminum (AA2024-O) was chosen as the working material. For elliptic, rectangular, and hexagonal tubes, the diameter of circular billet was 25 mm with a length of 25 mm. For the beginning of the process, the distance

between the punch and the billets was taken as 0.5 mm. The inside diameter of container in all cases was taken to be 0.4 mm greater than the billet diameter. The material properties for the simulated models were assumed as follows:

For AA2024-O (Ref 1)

$\bar{\sigma} = 292.77 * \bar{\varepsilon}^{0.15}$ (MPa)
$\rho = 2780$ (kg/m^3)
$E = 73.1$ (GPa)
$\varepsilon = 0.33$
$\sigma_y = 78.5$ (MPa)

The reduction of area was defined as:

$$RA\% = \frac{a}{A}(100),$$

where a is the section area of the punch and A is the section area of the billet.

Assumptions made in simulation were as follows:

(a) Material property for container and die were modeled as perfectly rigid.
(b) Interaction: tangential behavior
(c) Boundary conditions: Container movement was constrained in all directions; punch movement was constrained in all directions except the vertical direction.
(d) Type of element for the container was modeled as discrete rigid C3D8R
(e) Type of the element for punch was modeled as analytical rigid R3D4, a 4-node 3D bilinear rigid quadrilateral
(f) Element type for billet was modeled as deformable C3D8R, an 8-node linear brick.
(g) Adaptive meshing was chosen.

For example, for circular billet-elliptical punch:
Details of the elements are:

1. The upper face of billet in contact with the punch was partitioned on the basis of elliptic shape.
2. Element shape: hexahedral, technique: sweep
3. Number of nodes: 12,116
4. Number of elements: 10,800
5. 10,800 linear hexahedral elements of type C3D8R
6. Element library: Explicit, 3D stress
7. Geometric order: linear
8. Using ALE adaptive mesh domain: re-meshing sweep per element: 800,000, re-meshing sweep per increment: 3, initial re-meshing sweep value: 100
9. Element failure criteria: for all models, the optimum element size was obtained by trial and error until the worst aspect ratio (3) was achieved.

2.1 Mesh Convergence

To verify the mesh convergence for the results obtained from the finite element analysis, mesh convergence tests were carried out for each case. Here, a sample of these tests has been shown in Fig. 1. This test was carried out for the simulation of the backward extrusion of circular billet with an elliptical punch. A reduction of area of 36% and an aspect ratio of 1.25 was considered. It could be seen from the figure that around 26,500 elements the results converge. Similar tests were carried out for other simulations done in this work.

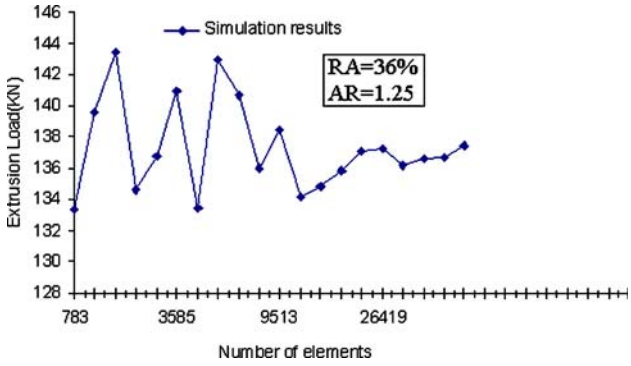

Fig. 1 Mesh convergence test for the backward extrusion of circular billet with an elliptical punch

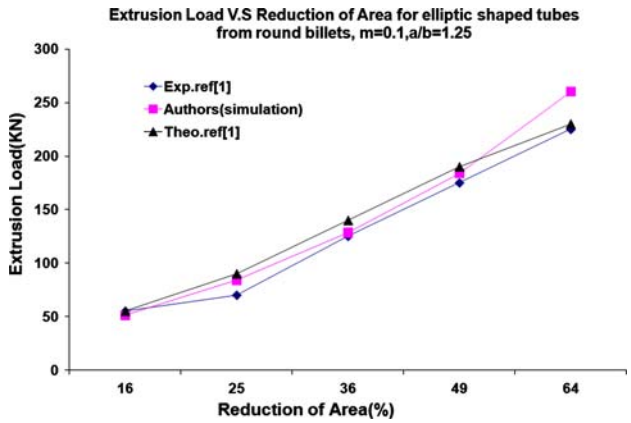

Fig. 2 Comparison of FEM simulation, theoretical, and experimental extrusion loads for different area reductions for the extrusion of internally elliptic-shaped tubes from round billets

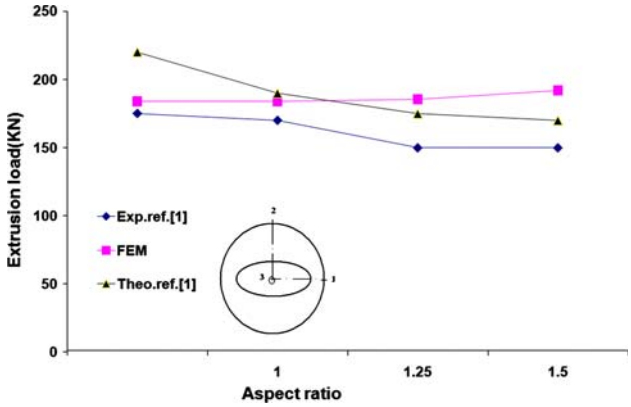

Fig. 3 Comparison of FEM simulation, theoretical, and experimental extrusion loads for different aspect ratios for the extrusion of internally elliptic-shaped tubes from round billets

3. Results and Discussion

Simulation of backward extrusion of internally elliptic, rectangular, and hexagonal sections from circular billets were carried out using ABAQUS FEM program. The results of these simulations are presented here. The results are presented according to the billet-punch shape.

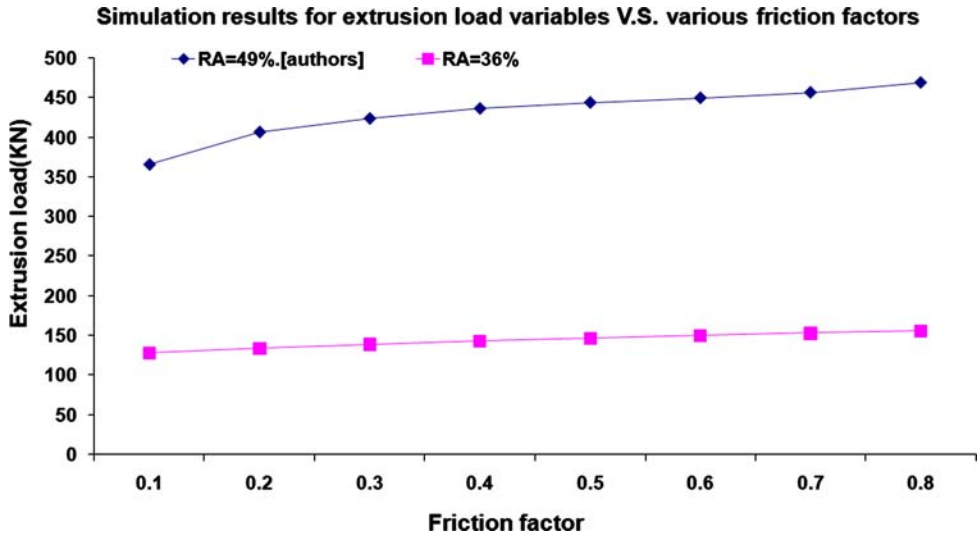

Fig. 4 FEM simulation results for the effect of friction factor on extrusion load for the extrusion of internally elliptic shapes from round billets

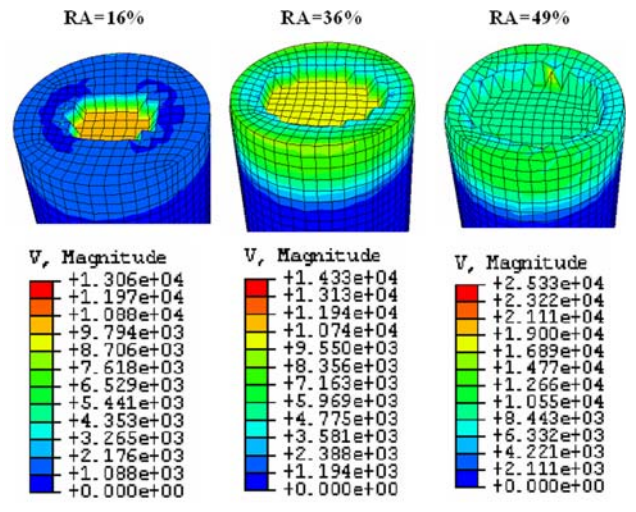

Fig. 5 Simulation results for the effect of area reduction on the configuration of the free surface and the velocity distribution of the extruded billet, m = 0.1, a/b = 1.25

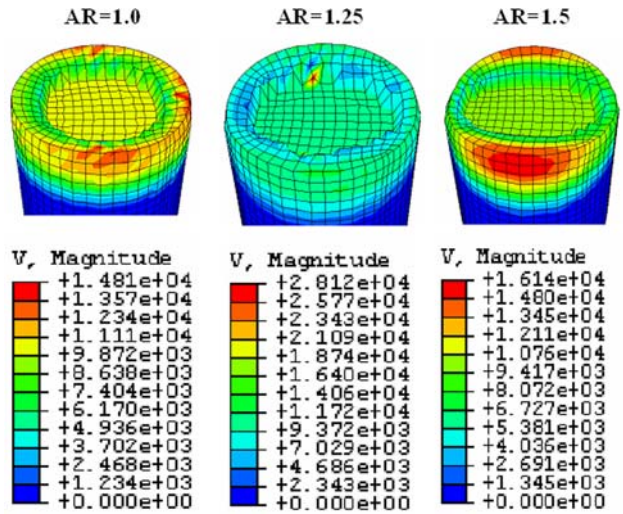

Fig. 6 Simulation results for the effect of aspect ratio on the configuration of the free surface and the velocity distribution of internally elliptic shaped tubes from circular billets, m = 0.1, RA = 49%

3.1 Circular Billet-Elliptic Punch

3.1.1 Extrusion Load. Figure 2 shows the effect of area reduction on the extrusion load for backward extrusion of internally elliptical-shaped tubes from round billets. The extrusion load increases with increasing reduction of area for a fixed aspect ratio and the given friction factor. FEM simulation results were compared with the experimental and theoretical values (Ref 1) and good agreements were found. For reduction of area of 36-49%, the extrusion loads were in good agreement with the experimental loads. The maximum difference between the value of the load obtained from the simulation and the experimental value was seen to be for the 64% area reduction.

The present simulation results for the extrusion load versus various aspect ratios in Fig. 3 are in good agreement with the experimental values and theoretical predictions (Ref 1). For aspect ratios of 1 to 1.3, the simulation results are closer to experimental ones.

Figure 4 shows the simulation results for the effect of friction factor on the extrusion load. For a given reduction of

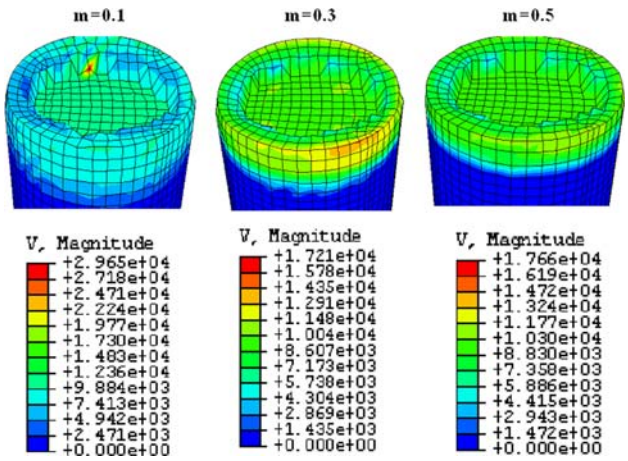

Fig. 7 Simulation results for the effect of friction factor on the configuration of the free surface and velocity field of internally elliptic-shaped tubes from circular billets, RA = 49%, a/b = 1.25

area and fixed aspect ratio, the extrusion load increases with the increase in the friction factor.

3.1.2 Distribution of Velocity and Configuration of the Free Surface of the Extruded Billet. The simulation results for the velocity distribution of the extruded billet are shown in Fig. 5 to 7 for different area reductions, aspect ratios, and friction factors, respectively. The effect of area reduction on the configuration of the free surface and velocity field contours of extruded billet for a given aspect ratio and the given friction factor are shown in Fig. 5.

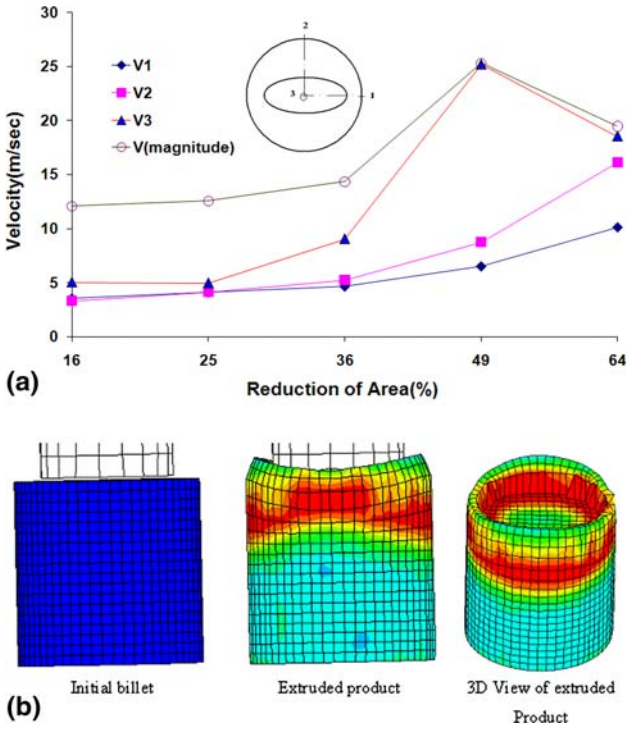

Fig. 8 (a) (a) Simulation results for reduction of area effect on velocity field. (b) Simulation results for grid deformation of RA = 64%, m = 0.1, *Aspect ratio* = 1.25

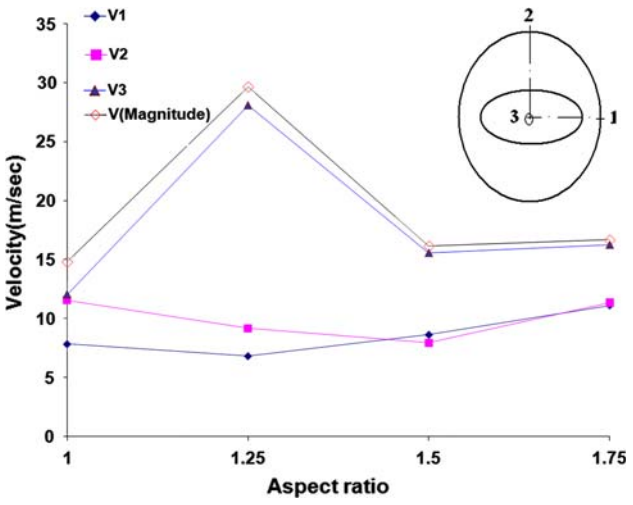

Fig. 9 Simulation results for aspect ratio effect on velocity field

Figure 6 shows the effect of aspect ratio on the configuration of the free surface and velocity field contribution of extruded billet for a fixed area reduction and the given friction factor.

In Fig. 7 are shown the effect of friction factor on the configuration of the free surface and velocity field for the extruded billet having a constant aspect ratio and reduction of area. Diagrams of the velocity variables versus various area reductions, aspect ratios, and friction factors are shown in Fig. 8 to 10, respectively.

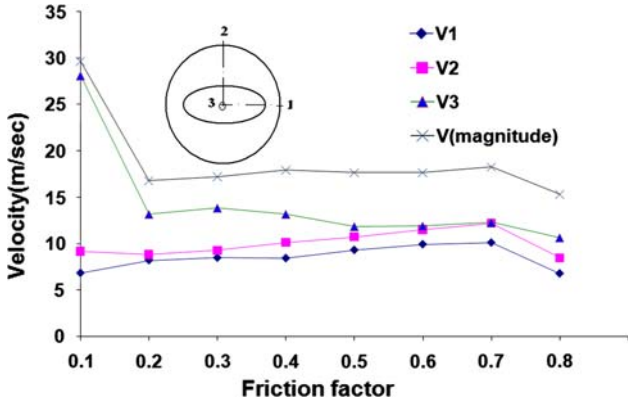

Fig. 10 Simulation results for friction factor effect on velocity field

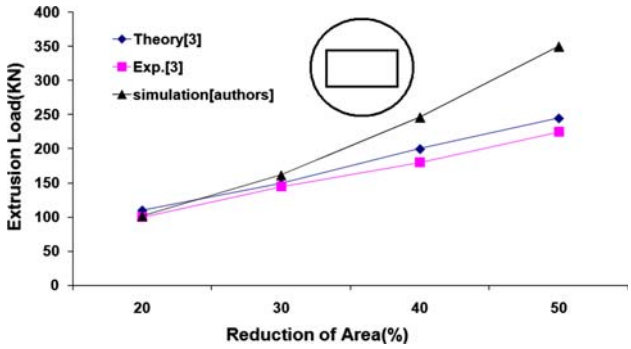

Fig. 11 Extrusion load variable vs. reduction of area for circular billet-rectangular punch, m = 0.1, a/b = 1.25

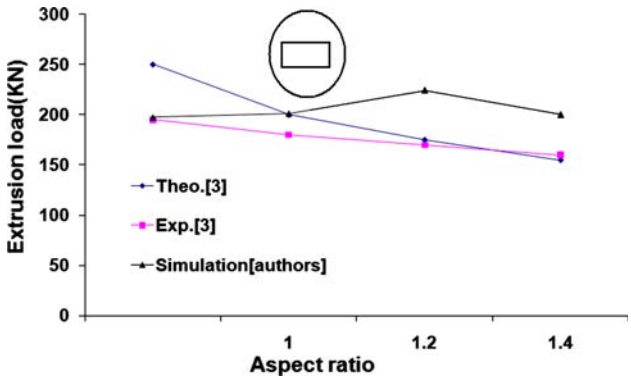

Fig. 12 Extrusion load variable vs. aspect ratio for circular billet-rectangular punch, m = 0.1, RA = 40%

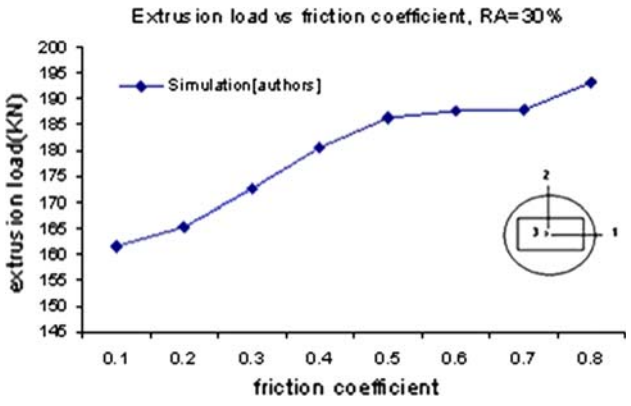

Fig. 13 Extrusion load vs. friction factor for backward extrusion simulation of internally rectangular sections from circular billets, a/b = 1.25

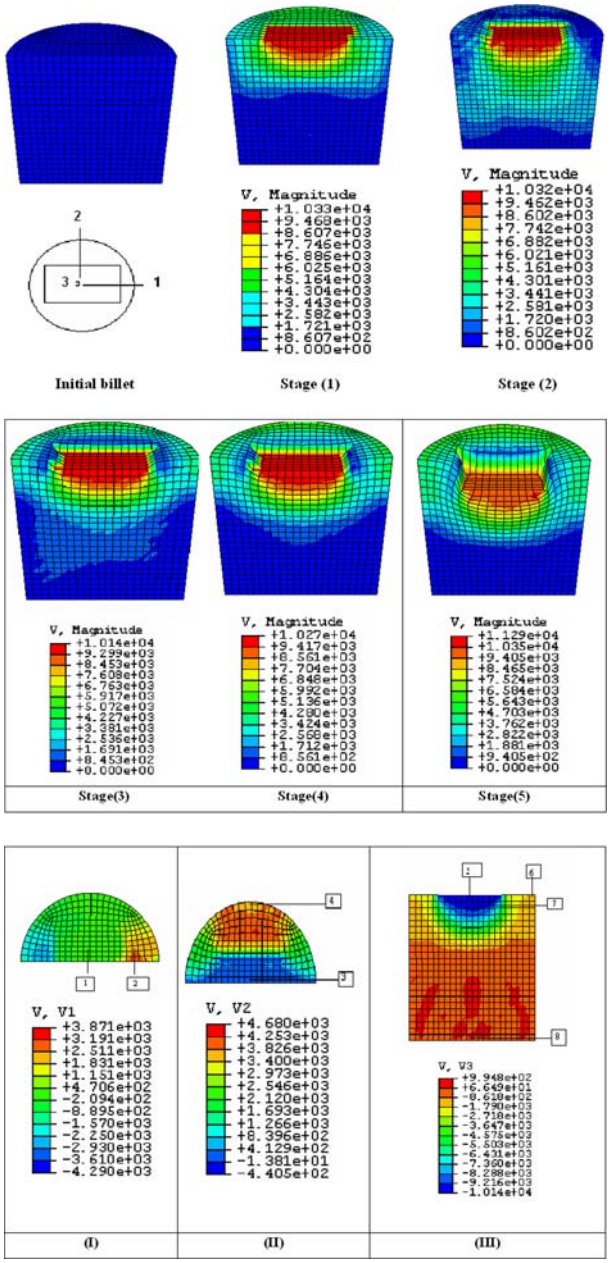

Fig. 14 Results of REM simulation for spatial velocity at nodes in circular billet-rectangular punch, m = 0.1, RA = 30%, a/b = 1.2

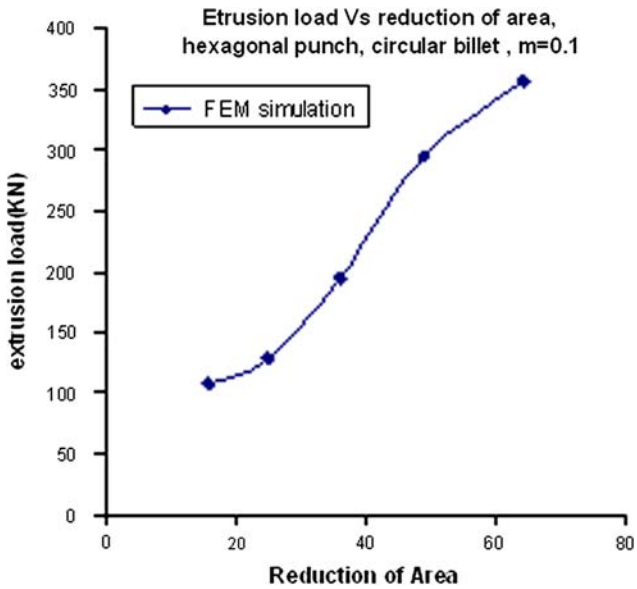

Fig. 15 Simulation results on effect of reduction of area on extrusion load

The diagram of velocity variables versus different area reductions for the same conditions has been shown in Fig. 8(a). For a reduction of area smaller than 25%, the velocity could be seen to decrease with increasing reduction of area and for values of reduction of area 25-64%, it could be seen that the velocity increases with increasing reductions of area. The results of simulation for RA = 25% to RA = 49% have been compared with theoretical predictions and experimental data for velocity field (Ref 1) and good agreement has been observed. Simulation results for grid deformation could be seen in Fig. 8(b). Because of thinning in the work piece wall for a RA = 64%, the material flows toward punch and is distorted excessively; therefore, the material flow encounters difficulties.

In Fig. 9, the effect of aspect ratio on the velocity has been shown. The variable rates of velocities for aspect ratios of 1.25 to 1.5 are trivial and for aspect ratios of 1.5 to A.R = 1.75, the velocity has decreased.

In Fig. 10, the effect of the friction factor on the velocity field has been shown. Except for m = 0.1 to 0.2, there seems to be no appreciable difference between the two cases.

3.2 Circular Billet-Rectangular Punch Results

3.2.1 Extrusion Load. Figures 11 to 14 show the results of FEM simulation for internally rectangular sections from round billets. In Fig. 11, a graph of extrusion load versus reduction of area is given for the backward extrusion of internally rectangular sections from circular billets. Comparison of other theoretical and experimental results with the FEM simulation of the authors is also seen in this figure. Authors' results show better agreement with the experimental values at lower values of the reduction of area.

In Fig. 12, a graph of extrusion load versus aspect ratio is given for the backward extrusion of internally rectangular sections from circular billets. Authors' results show better agreement with the experimental values at lower values of aspect ratio.

In Fig. 13, a graph of extrusion load versus friction factor for the backward extrusion simulation of internally rectangular

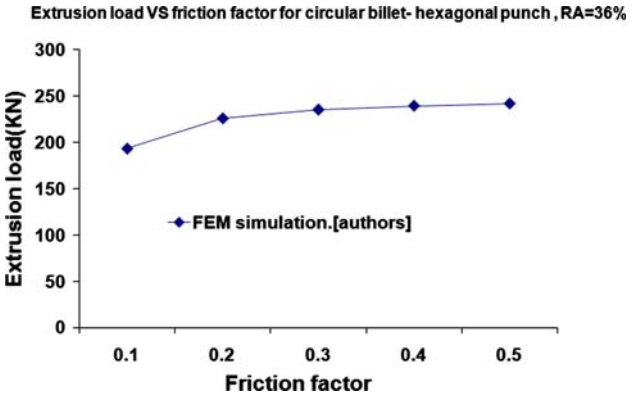

Fig. 16 Effect of friction factor on extrusion load

sections from circular billets is shown. The extrusion load increases with increasing friction factor. With increasing friction factor the amount of friction force increases and this force causes the total load required for the process to increase.

3.2.2 Velocity Field Distribution. For the same extrusion, the grid deformation and spatial velocity distribution at nodes are also given in Fig. 14. Starting from the initial stage of the extrusion process and going through to the end, five different stages are observed. The values of velocity distributions in the part are also shown for each stage. The velocity field is shown by three directional velocities: $V1$, $V2$, and $V3$. The magnified figure of one stage for contour distribution of $V1$, $V2$, and $V3$ is shown in Fig. 14(I-III), respectively. The values of $V1$ were greater at locations nearer to the punch

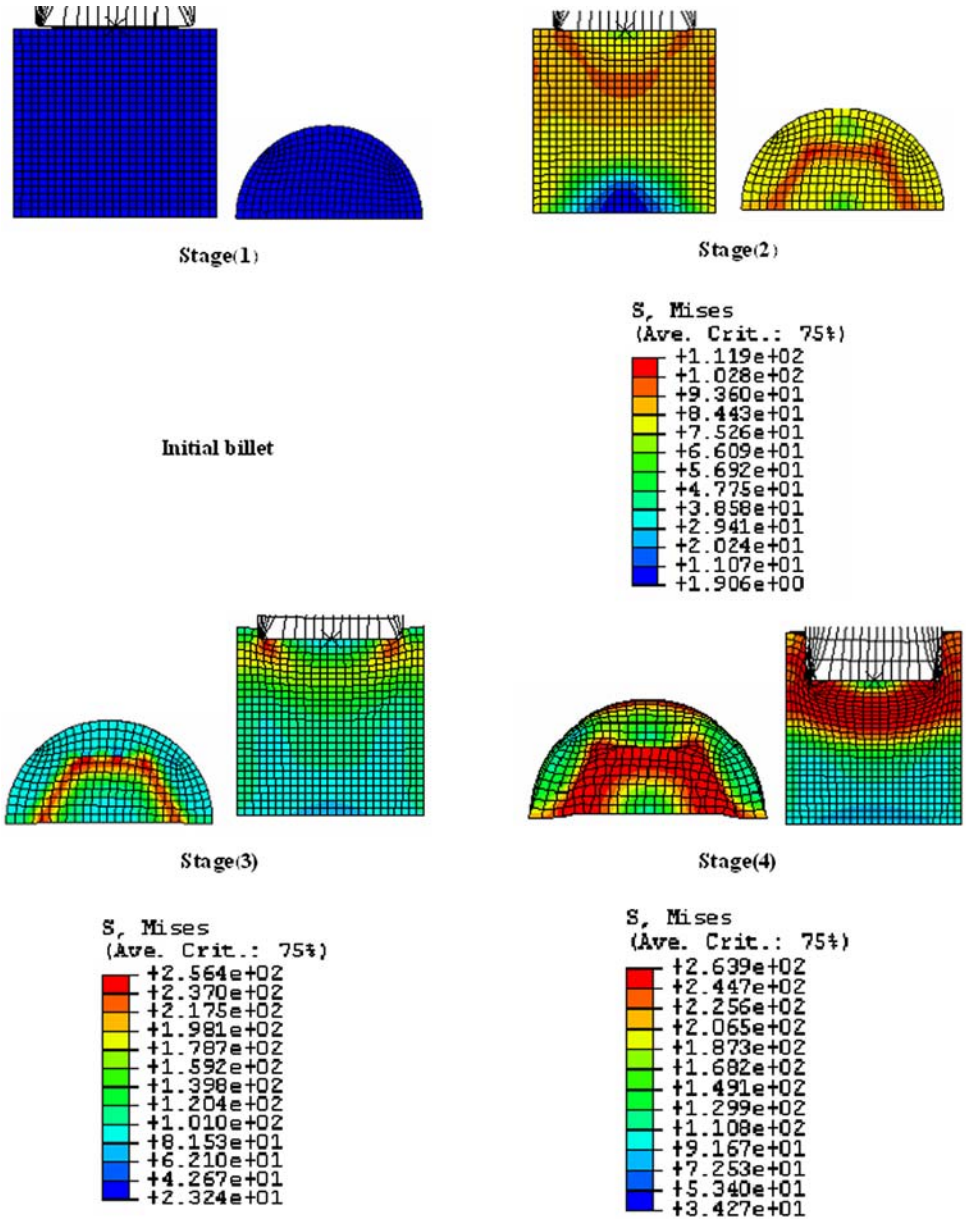

Fig. 17 Distribution of stress in backward extrusion simulation of internally hexagonal shapes from round billets, RA = 49%, Material: AA2024-O

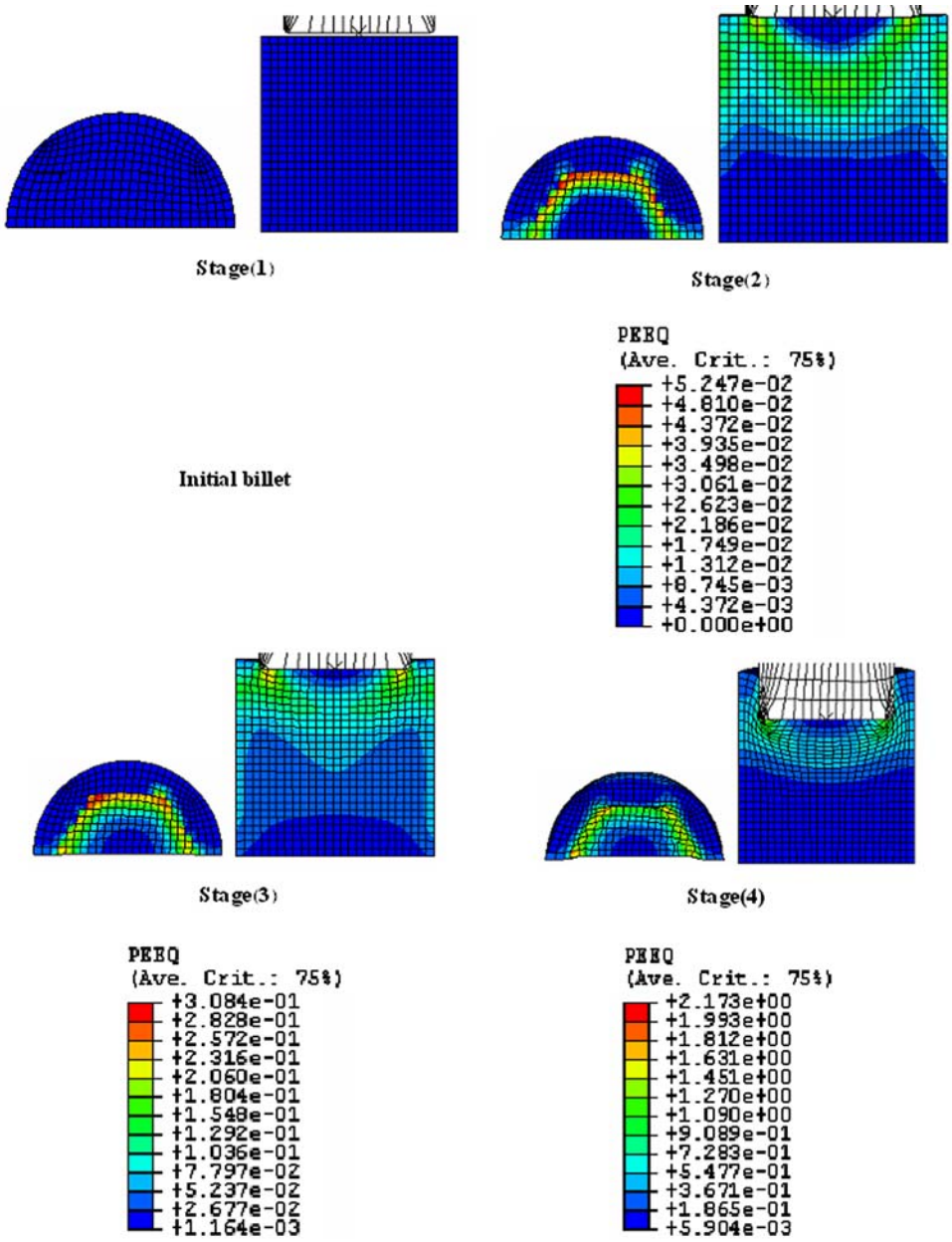

Fig. 18 Distribution of plastic equivalent strain in backward extrusion simulation of internally hexagonal shapes from round billets, *RA* = 49%, Material: AA2024-O

corner than elsewhere and it is lowest at the center of free surface of the extruded part at position (1). Also, *V*1 decreases from position (1) to (2), for the nodes near the wall of container.

Values of *V*2 were greater at locations (3) and (4) and between these sections, *V*2 has the lowest value. The value of *V*3 was greatest at position (5) and decreases as one move toward (6), for the nodes of the work piece near the container wall. From position (7), near the free surface of workpiece toward position (8), for the nodes near the container lower section, *V*3 decreases gradually. These results were not obtained by other methods in other references.

3.3 Circular Billet-Hexagonal Punch Results

3.3.1 Extrusion Load. In Fig. 15 to 18 are shown simulation results for backward extrusion of internally hexagonal sections from circular billets. In Fig. 15, a graph of extrusion load versus reduction of area is given for the backward extrusion of internally hexagonal sections from circular billets. In Fig. 16, a graph of extrusion load versus friction factor for the backward extrusion of internally hexagonal sections from circular billets is shown. The extrusion load increases with increasing friction factor.

3.3.2 Stress and Strain Distribution. For the same extrusion, the grid deformation and stress distribution are also given in Fig. 17. Starting from the initial stage of the extrusion process and going through to the end, four different stages are observed. The values of stress distribution in the part are also shown for each stage. A reduction of area of 49% was used for these simulations. It is illustrated that in which part of the billet the stress is greatest.

The results for the equivalent strain distribution for the backward extrusion of internally hexagonal and externally

circular shapes are shown in Fig. 18 for the four stages of the simulation. It could be seen that, as expected, the highest values occur at where the highest deformation is. As shown in these stages, because of maximum deformation in the surface of the work piece which is in contact with the corner of the punch, the plastic equivalent effective strain is greater than elsewhere. Also, in the initial stage of the process, contours of strains are distributed in broad areas and gradually decrease through the end of the process. Because, in the initial stage, with increasing stress, the plastic area develops and includes larger regions of the billet. However, after material flows and plastic deformation develops further, the deformation area is fixed and strains confine in the plastic areas. It should be mentioned that these results are very similar to those given in Ref 2.

4. Conclusions

Finite element simulation of the backward extrusion process was carried out for the internally elliptical, rectangular, and hexagonal and externally circular sections. The results for the elliptic tubes obtained from 3D simulation showed good agreement with the previous work. The 3D velocity field distribution and the free surface configurations obtained by the authors showed very good agreement with the experimental evidence and much improved over the previous work. The 3D simulation predictions for the extrusion force for lower reduction of areas were closer to experimental observations whereas for higher reductions they were further apart. Some results such as the velocity distribution during different stages of the extrusion process for rectangular tubes and other results such as extrusion load, stress, and strain distribution for hexagonal tubes were also obtained which were not given in the previous work.

References

1. W.B. Bae and D.Y. Yang, An Upper-Bound Analysis of the Backward Extrusion of Internally Elliptic-Shaped Tubes from Round Billets, *J. Mater. Process. Technol.*, 1992, **30**(1–2), p 13–20
2. W.B. Bae and D.Y. Yang, An Analysis of Backward Extrusion of Internally Circular-Shaped Tubes from Arbitrarily-Shaped Billets by the Upper-Bound Method, *J. Mater. Process. Technol.*, 1993, **36**(2), p 175–185
3. W.B. Bae and D.Y. Yang, An Upper-Bound Analysis of the Backward Extrusion of Tubes of Complicated Internal Shapes from Round Billets, *J. Mater. Process. Technol.*, 1993, **36**(2), p 157–173
4. R.-S. Lee and C.-T. Kwan, A Modified Analysis of the Backward Extrusion of Internally Circular-Shaped Tubes from Arbitrarily Shaped Billets by the Upper-Bound Elemental Technique, *J. Mater. Process. Technol.*, 1996, **59**, p 351–358
5. Y.T. Lin and J.P. Wang, A New Upper-Bound Elemental Technique Approach, *J. Comput. Struct.*, 1997, **65**(4), p 601–611
6. M.M. Moshksar and R. Ebrahim, An Analytical Approach for Backward Extrusion Forging of Regular Polygonal Hollow Components, *Int. J. Mech. Sci.*, 1998, **40**(12), p 1247–1263
7. Y.M. Guo, Y. Yokouchi, and K. Nakanishi, Hot Backward Extrusion Comparative Analyses by a Combined Finite Element Method, *Int. J. Mech. Sci.*, 2000, **42**, p 1867–1885
8. K. Abrinia and S. Orangi, A Finite Element Simulation for the Backward Extrusion of Internally Hollow Circular Sections from Polygonal Billets, *J. Fac. Eng. Univ. Tehran (special issue on: Mechanical Engineering)*, 2007, **40**(6), p 771–780